

## Stable bound states of $N$ 's, $\Lambda$ 's and $\Xi$ 's

H. Garcilazo

*Escuela Superior de Física y Matemáticas,  
Instituto Politécnico Nacional, Edificio 9, 07738 México D.F., Mexico.  
e-mail: humberto@esfm.ipn.mx*

A. Valcarce

*Departamento de Física Fundamental and IUFFyM,  
Universidad de Salamanca, E-37008 Salamanca, Spain.  
e-mail: valcarce@usal.es*

J. Vijande

*Unidad Mixta de Investigación en Radiofísica e Instrumentación Nuclear en Medicina,  
Instituto de Investigación Sanitaria La Fe (IIS-La Fe)-Universitat de  
Valencia (UV) and IFIC (UV-CSIC), Valencia, Spain.  
e-mail: javier.vijande@uv.es*

Received 21 April 2017; accepted 9 June 2017

We review our recent work about the stability of strange few-body systems containing  $N$ 's,  $\Lambda$ 's, and  $\Xi$ 's. We make use of local central Yukawa-type Malfliet-Tjon interactions reproducing the low-energy parameters and phase shifts of the nucleon-nucleon system and the latest updates of the hyperon-nucleon and hyperon-hyperon ESC08c Nijmegen potentials. We solve the three- and four-body bound-state problems by means of Faddeev equations and a generalized Gaussian variational method, respectively. The hypertriton,  $\Lambda np$  ( $I$ ) $J^P = (1/2)1/2^+$ , is bound by 144 keV; the recently discussed  $\Lambda nn$  ( $I$ ) $J^P = (1/2)1/2^+$  system is unbound, as well as the  $\Lambda\Lambda nn$  ( $I$ ) $J^P = (1)0^+$  system, being just above threshold. Our results indicate that the  $\Xi NN$ ,  $\Xi\Xi N$  and  $\Xi\Xi NN$  systems with maximal isospin might be bound.

*Keywords:* Baryon-Baryon interactions; Faddeev equations; variational approaches.

PACS: 21.45.-v; 25.10.+s; 11.80.Jy

### 1. Introduction

Strange nuclear physics is a very topical subject. The hyperon-nucleon ( $YN$ ) and hyperon-hyperon ( $YY$ ) interactions constitute the input for microscopic calculations of few- and many-body systems involving strangeness, such as exotic neutron star matter [1–5] or hypernuclei [6–8]. There are theoretical debates [9–14] on the possible existence of a neutral bound state of two neutrons and a  $\Lambda$  hyperon,  ${}^3_\Lambda n$ , suggested by recent data of the HyPHI Collaboration [15]. There have been also recent proposals regarding the stability of  ${}^4_{\Lambda\Lambda} n$  [14], the existence of  $\Xi$  hypernuclei [6–8], or the existence of a strangeness  $-2$  hypertriton [16, 17]. Obviously, all these predictions are subject to the uncertainties of our knowledge of the baryon-baryon interaction, in particular in the strangeness  $-2$  sector. Experimentally, it has been recently reported an emulsion event, the so-called KISO event, providing evidence of a possible deeply bound state of  $\Xi^- - {}^{14}\text{N}$  [18]. Although microscopic calculations are impossible in this case and, consequently, their interpretation will be always affected by uncertainties, the ESC08c Nijmegen potential has been recently updated [19–21] to give account for the most recent experimental information of the strangeness  $-2$  sector, the KISO [18] and the NAGARA [22] events. A thorough discussion of the present status of the experimental and theoretical progress in hypernuclear physics can be found in Refs. 23 and 24.

When a two-baryon interaction is attractive, if the system is merged with nuclear matter and the Pauli principle does not impose severe restrictions, the attraction may be reinforced. Simple examples of the effect of a third or a fourth baryon in two-baryon systems could be given. The deuteron, ( $I$ ) $J^P = (0)1^+$ , is bound by 2.225 MeV, while the triton, ( $I$ ) $J^P = (1/2)1/2^+$ , is bound by 8.480 MeV, and the  $\alpha$  particle, ( $I$ ) $J^P = (0)0^+$ , is bound by 28.295 MeV. The binding per nucleon  $B/A$  increases as  $1 : 3 : 7$ . A similar argument could be employed for strangeness  $-1$  systems. Whereas the existence of dibaryon states is still under discussion<sup>i</sup>, the hypertriton  ${}^3_\Lambda \text{H}$ , ( $I$ ) $J^P = (0)1/2^+$ , is bound with a separation energy of  $130 \pm 50$  keV, and the  ${}^4_\Lambda \text{H}$ , ( $I$ ) $J^P = (0)0^+$ , is bound with a separation energy of  $2.12 \pm 0.01$  (stat)  $\pm 0.09$  (syst) MeV [26]. This cooperative effect of the attraction in the two-body subsystems when merged in few-baryon states was also made evident in the prediction of a  $\Sigma NN$  quasibound state in the ( $I$ ) $J^P = (1)1/2^+$  channel very near threshold [27, 28]. Such  $\Sigma NN$  quasibound state has been recently suggested in  ${}^3\text{He}(\text{K}^-, \pi^\mp)$  reactions at 600 MeV/c [29].

In this paper, we review our recent studies of the three-body systems:  $\Lambda NN$ ,  $\Xi NN$ ,  $\Lambda\Lambda N$ , and  $\Xi\Xi N$ , as well as the four-body systems  $\Xi\Xi NN$  and  $\Lambda\Lambda NN$ . We make use of the most recent updates of the ESC08c Nijmegen potentials in the strangeness  $-1$ ,  $-2$ ,  $-3$  and  $-4$  sec-

tor [19, 20, 30] accounting for the recent KISO [18] and NA-GARA [22] events in the strangeness  $-2$  sector. As discussed above, the existence of two-body attractive interactions or bound states could give rise to other stable few-body systems when merged with other nucleons or hyperons. For example, the overall attractive character of the  $\Xi N$  interaction comes suggested by recent preliminary results from lattice QCD [31] together with other indications of certain emulsion data [20, 21, 30]. Besides the recent update of ESC08c Nijmegen model,  $\Xi$ -hypernuclear calculations [32] and chiral quark models [33] found a  $\Xi N$  attractive interaction before the KISO event. Furthermore, the possible existence of stable strange few-body states comes reinforced by the attractive character of the  $\Xi\Xi$  interaction for some partial waves [19, 30, 34–38]. It is worth to mention that preliminary studies of the  $\Xi\Xi N$  system [39] indicate that lattice QCD calculations of multibaryon systems are now within sight. Analogously, if a second  $\Lambda$  would be added to the uncertain  $\Lambda nn$  state, the weakly attractive  $\Lambda\Lambda$  interaction [22] and the reinforcement of the  $\Lambda N$  potential without paying a price for antisymmetry requirements, may give rise to a stable bound state [14].

One should bear in mind how delicate is the few-body problem in the regime of weak binding, as demonstrated in Ref. 40 for the  ${}^4_{\Lambda\Lambda}\text{H}$  system. Besides, there are models for the  $YN$  interaction, like the hybrid quark-model based analysis of Ref. 41, the effective field theory approach of Ref. 42, or even some of the earlier models of the Nijmegen group [34] that, in general, predict interactions weakly attractive or repulsive. One does not expect that these models will give rise to stable three- or four-body states. However, it is worth to emphasize that current hypernuclei studies [6–8, 32, 40] have been performed by means of interactions derived from the Nijmegen models and, thus, the present review complements such previous work for the simplest systems that can be studied exactly. To advance in the knowledge of the details of the  $YN$  interaction, high-resolution spectroscopy of  $\Xi$  hypernuclei using  ${}^{12}\text{C}$  targets in  $(K^-, K^+)$  reactions has been awaited [43, 44] and it is now planned at J-PARC [45]. The new hybrid experiment  $E07$  recently approved at J-PARC is expected to record of the order of  $10^4$   $\Xi^-$  stopping events [46], one order of magnitude larger than the previous  $E373$  experiment, and will hopefully clarify the phenomenology of some of the systems studied in the present work.

The review is organized as follows. In Sec. 2 we describe the technical details to solve the three-body bound state Faddeev equations as well as the generalized Gaussian variational method used to look for bound states of the four-body problem. In Sec. 3 we construct the two-body amplitudes needed for the solution of the bound state three- and four-body problems. The results are presented and discussed in Sec. 4. Finally, in Sec. 5 we summarize our main conclusions.

## 2. The three- and four-body bound-state problems

In this section we outline the solution of the three- and four-body bound-state problems. We will restrict ourselves to configurations where all particles are in  $S$ -wave states. The three-body problem has been widely discussed in the literature and we refer the reader to Refs. 47 to 49 for a more detailed discussion. The Faddeev equations for a system with total isospin  $I$  and total spin  $J$  are,

$$T_{i;IJ}^{i_i j_i}(p_i q_i) = \sum_{j \neq i} \sum_{i_j j_j} h_{i_j j_j}^{i_i j_i; i_j j_j} \frac{1}{2} \int_0^\infty q_j^2 dq_j \times \int_{-1}^1 d\cos\theta t_{i; i_j j_i}(p_i, p'_i; E - q_i^2/2\nu_i) \times \frac{1}{E - p_j^2/2\mu_j - q_j^2/2\nu_j} T_{j;IJ}^{i_j j_j}(p_j q_j), \quad (1)$$

where  $t_{i; i_j j_i}$  stands for the two-body amplitudes with isospin  $i_i$  and spin  $j_i$ .  $p_i$  is the momentum of the pair  $jk$  (with  $ijk$  an even permutation of 123) and  $q_i$  the momentum of particle  $i$  with respect to the pair  $jk$ .  $\mu_i$  and  $\nu_i$  are the corresponding reduced masses, and  $h_{i_j j_j}^{i_i j_i; i_j j_j}$  are spin-isospin coefficients.

Expanding the amplitude  $t_{i; i_j j_i}(x_i, x'_i; e)$  in terms of Legendre polynomials, Eq. (1) can be written as,

$$T_{i;IJ}^{i_i j_i}(x_i q_i) = \sum_n P_n(x_i) T_{i;IJ}^{n i_j j_i}(q_i), \quad (2)$$

where  $T_{i;IJ}^{n i_j j_i}(q_i)$  satisfies the one-dimensional integral equation,

$$T_{i;IJ}^{n i_j j_i}(q_i) = \sum_{j \neq i} \sum_{m i_j j_j} \int_0^\infty dq_j A_{i_j j_j}^{n i_j j_i; m i_j j_j} \times (q_i, q_j; E) T_{j;IJ}^{m i_j j_j}(q_j), \quad (3)$$

with

$$A_{i_j j_j}^{n i_j j_i; m i_j j_j}(q_i, q_j; E) = h_{i_j j_j}^{i_i j_i; i_j j_j} \sum_r \tau_{i; i_j j_i}^{nr}(E - q_i^2/2\nu_i) \frac{q_j^2}{2} \times \int_{-1}^1 d\cos\theta \frac{P_r(x'_i) P_m(x_j)}{E - p_j^2/2\mu_j - q_j^2/2\nu_j}. \quad (4)$$

The four-body problem has been addressed by means of the variational method, specially suited for studying low-lying states. The nonrelativistic hamiltonian is given by,

$$H = \sum_{i=1}^4 \left( m_i + \frac{\vec{p}_i^2}{2m_i} \right) + \sum_{i < j=1}^4 V(\vec{r}_{ij}), \quad (5)$$

where the potential  $V(\vec{r}_{ij})$  corresponds to an arbitrary two-body interaction.

The variational wave function must include all possible spin-isospin channels contributing to a given configuration. For each channel  $s$ , the wave function will be the tensor product of a spin ( $|S_{s_1}\rangle$ ), isospin ( $|I_{s_2}\rangle$ ), and radial ( $|R_{s_3}\rangle$ ) component,

$$|\phi_s\rangle = |S_{s_1}\rangle \otimes |I_{s_2}\rangle \otimes |R_{s_3}\rangle, \quad (6)$$

where  $s \equiv \{s_1, s_2, s_3\}$ . Once the spin and isospin parts are integrated out, the coefficients of the radial wave function are obtained by solving the system of linear equations,

$$\sum_{s'} \sum_s \beta_{s_3}^i \langle R_{s_3}^j | H | R_{s_3}^i \rangle - E \langle R_{s_3}^j | R_{s_3}^i \rangle \delta_{s,s'} = 0 \quad \forall j, \quad (7)$$

where the eigenvalues are obtained by a minimization procedure.

For the description of the four-body wave function we consider the Jacobi coordinates:

$$\begin{aligned} \vec{r}_{NN} &= \vec{x} = \vec{r}_1 - \vec{r}_2, \\ \vec{r}_{YY} &= \vec{y} = \vec{r}_3 - \vec{r}_4, \\ \vec{r}_{NN-YY} &= \vec{z} = \frac{1}{2}(\vec{r}_1 + \vec{r}_2) - \frac{1}{2}(\vec{r}_3 + \vec{r}_4), \\ \vec{R}_{CM} &= \vec{R} = \frac{\sum m_i \vec{r}_i}{\sum m_i}, \end{aligned} \quad (8)$$

The total wave function should have well-defined permutation properties under the exchange of identical particles. The spin part can be written as,

$$[(s_1 s_2)_{S_{12}} (s_3 s_4)_{S_{34}}]_S \equiv |S_{12} S_{34}\rangle_S, \quad (9)$$

where the spin of the two  $N$ 's ( $Y$ 's) is coupled to  $S_{12}$  ( $S_{34}$ ). Two identical spin-1/2 fermions in a  $S = 0$  state are antisymmetric ( $A$ ) under permutations while those coupled to  $S = 1$  are symmetric ( $S$ ). We summarize in Table I the corresponding vectors for each total spin together with their symmetry properties<sup>ii</sup>

TABLE I. Spin basis vectors for all possible total spin states ( $S$ ). The 'Symmetry' column stands for the symmetry properties of the pair of identical particles.

| $S$ | Vector         | Symmetry |
|-----|----------------|----------|
| 0   | $ 00\rangle_S$ | AA       |
|     | $ 11\rangle_S$ | SS       |
| 1   | $ 01\rangle_S$ | AS       |
|     | $ 10\rangle_S$ | SA       |
|     | $ 11\rangle_S$ | SS       |
| 2   | $ 11\rangle_S$ | SS       |

The most general radial wave function with total orbital angular momentum  $L = 0$  may depend on the six scalar quantities that can be constructed with the Jacobi coordinates of the system, they are:  $\vec{x}^2, \vec{y}^2, \vec{z}^2, \vec{x} \cdot \vec{y}, \vec{x} \cdot \vec{z},$  and  $\vec{y} \cdot \vec{z}$ . We define the variational spatial wave function as a linear combination of *generalized Gaussians*,

$$|R_{s_3}\rangle = \sum_{i=1}^n \beta_{s_3}^i R_{s_3}^i(\vec{x}, \vec{y}, \vec{z}) = \sum_{i=1}^n \beta_{s_3}^i R_{s_3}^i, \quad (10)$$

where  $n$  is the number of Gaussians used for each spin-isospin component.  $R_{s_3}^i$  depends on six variational parameters:  $a_s^i, b_s^i, c_s^i, d_s^i, e_s^i,$  and  $f_s^i$ , one for each scalar quantity. Therefore, the four-body system will depend on  $6 \times n \times n_s$  variational parameters, where  $n_s$  is the number of different channels allowed by the Pauli principle. Eq. (10) should have well-defined permutation symmetry under the exchange of both  $N$ 's and  $Y$ 's,

$$P_{12}(\vec{x} \rightarrow -\vec{x}) R_{s_3}^i = P_x R_{s_3}^i \quad (11)$$

$$P_{34}(\vec{y} \rightarrow -\vec{y}) R_{s_3}^i = P_y R_{s_3}^i,$$

where  $P_x$  and  $P_y$  are  $-1$  for antisymmetric states, ( $A$ ), and  $+1$  for symmetric ones, ( $S$ ). Thus, one can build the following radial combinations,  $(P_x P_y) = (SS), (SA), (AS),$  and  $(AA)$ :

$$\begin{aligned} (SS) \Rightarrow R_1^i &= \text{Exp}(-a_s^i \vec{x}^2 - b_s^i \vec{y}^2 - c_s^i \vec{z}^2 - d_s^i \vec{x} \cdot \vec{y} - e_s^i \vec{x} \cdot \vec{z} - f_s^i \vec{y} \cdot \vec{z}) \\ &+ \text{Exp}(-a_s^i \vec{x}^2 - b_s^i \vec{y}^2 - c_s^i \vec{z}^2 + d_s^i \vec{x} \cdot \vec{y} - e_s^i \vec{x} \cdot \vec{z} + f_s^i \vec{y} \cdot \vec{z}) \\ &+ \text{Exp}(-a_s^i \vec{x}^2 - b_s^i \vec{y}^2 - c_s^i \vec{z}^2 + d_s^i \vec{x} \cdot \vec{y} + e_s^i \vec{x} \cdot \vec{z} - f_s^i \vec{y} \cdot \vec{z}) \\ &+ \text{Exp}(-a_s^i \vec{x}^2 - b_s^i \vec{y}^2 - c_s^i \vec{z}^2 - d_s^i \vec{x} \cdot \vec{y} + e_s^i \vec{x} \cdot \vec{z} + f_s^i \vec{y} \cdot \vec{z}), \end{aligned} \quad (12)$$

$$\begin{aligned} (SA) \Rightarrow R_2^i &= \text{Exp}(-a_s^i \vec{x}^2 - b_s^i \vec{y}^2 - c_s^i \vec{z}^2 - d_s^i \vec{x} \cdot \vec{y} - e_s^i \vec{x} \cdot \vec{z} - f_s^i \vec{y} \cdot \vec{z}) \\ &- \text{Exp}(-a_s^i \vec{x}^2 - b_s^i \vec{y}^2 - c_s^i \vec{z}^2 + d_s^i \vec{x} \cdot \vec{y} - e_s^i \vec{x} \cdot \vec{z} + f_s^i \vec{y} \cdot \vec{z}) \\ &+ \text{Exp}(-a_s^i \vec{x}^2 - b_s^i \vec{y}^2 - c_s^i \vec{z}^2 + d_s^i \vec{x} \cdot \vec{y} + e_s^i \vec{x} \cdot \vec{z} - f_s^i \vec{y} \cdot \vec{z}) \\ &- \text{Exp}(-a_s^i \vec{x}^2 - b_s^i \vec{y}^2 - c_s^i \vec{z}^2 - d_s^i \vec{x} \cdot \vec{y} + e_s^i \vec{x} \cdot \vec{z} + f_s^i \vec{y} \cdot \vec{z}), \end{aligned} \quad (13)$$

$$\begin{aligned}
 (AS) \Rightarrow R_3^i &= \text{Exp}(-a_s^i \bar{x}^2 - b_s^i \bar{y}^2 - c_s^i \bar{z}^2 - d_s^i \bar{x} \cdot \bar{y} - e_s^i \bar{x} \cdot \bar{z} - f_s^i \bar{y} \cdot \bar{z}) \\
 &+ \text{Exp}(-a_s^i \bar{x}^2 - b_s^i \bar{y}^2 - c_s^i \bar{z}^2 + d_s^i \bar{x} \cdot \bar{y} - e_s^i \bar{x} \cdot \bar{z} + f_s^i \bar{y} \cdot \bar{z}) \\
 &- \text{Exp}(-a_s^i \bar{x}^2 - b_s^i \bar{y}^2 - c_s^i \bar{z}^2 + d_s^i \bar{x} \cdot \bar{y} + e_s^i \bar{x} \cdot \bar{z} - f_s^i \bar{y} \cdot \bar{z}) \\
 &- \text{Exp}(-a_s^i \bar{x}^2 - b_s^i \bar{y}^2 - c_s^i \bar{z}^2 - d_s^i \bar{x} \cdot \bar{y} + e_s^i \bar{x} \cdot \bar{z} + f_s^i \bar{y} \cdot \bar{z}),
 \end{aligned} \tag{14}$$

$$\begin{aligned}
 (AA) \Rightarrow R_4^i &= \text{Exp}(-a_s^i \bar{x}^2 - b_s^i \bar{y}^2 - c_s^i \bar{z}^2 - d_s^i \bar{x} \cdot \bar{y} - e_s^i \bar{x} \cdot \bar{z} - f_s^i \bar{y} \cdot \bar{z}) \\
 &- \text{Exp}(-a_s^i \bar{x}^2 - b_s^i \bar{y}^2 - c_s^i \bar{z}^2 + d_s^i \bar{x} \cdot \bar{y} - e_s^i \bar{x} \cdot \bar{z} + f_s^i \bar{y} \cdot \bar{z}) \\
 &- \text{Exp}(-a_s^i \bar{x}^2 - b_s^i \bar{y}^2 - c_s^i \bar{z}^2 + d_s^i \bar{x} \cdot \bar{y} + e_s^i \bar{x} \cdot \bar{z} - f_s^i \bar{y} \cdot \bar{z}) \\
 &+ \text{Exp}(-a_s^i \bar{x}^2 - b_s^i \bar{y}^2 - c_s^i \bar{z}^2 - d_s^i \bar{x} \cdot \bar{y} + e_s^i \bar{x} \cdot \bar{z} + f_s^i \bar{y} \cdot \bar{z}).
 \end{aligned} \tag{15}$$

The last equations can be expressed in a compact manner by defining the following function,

$$\begin{aligned}
 g(s_1, s_2, s_3) &= \text{Exp}(-a_s^i \bar{x}^2 - b_s^i \bar{y}^2 - c_s^i \bar{z}^2 \\
 &- s_1 d_s^i \bar{x} \cdot \bar{y} - s_2 e_s^i \bar{x} \cdot \bar{z} - s_3 f_s^i \bar{y} \cdot \bar{z}),
 \end{aligned} \tag{16}$$

and the vectors

$$\vec{G}_s^i = \begin{pmatrix} g(+, +, +) \\ g(-, +, -) \\ g(-, -, +) \\ g(+, -, -) \end{pmatrix}, \tag{17}$$

and

$$\begin{aligned}
 \vec{\alpha}_{SS} &= (+, +, +, +) \\
 \vec{\alpha}_{SA} &= (+, -, +, -) \\
 \vec{\alpha}_{AS} &= (+, +, -, -) \\
 \vec{\alpha}_{AA} &= (+, -, -, +),
 \end{aligned} \tag{18}$$

which allows to write Eqs. (13)–(15) as,

$$\begin{aligned}
 (SS) \Rightarrow R_1^i &= \vec{\alpha}_{SS} \cdot \vec{G}_s^i \\
 (SA) \Rightarrow R_2^i &= \vec{\alpha}_{SA} \cdot \vec{G}_s^i \\
 (AS) \Rightarrow R_3^i &= \vec{\alpha}_{AS} \cdot \vec{G}_s^i \\
 (AA) \Rightarrow R_4^i &= \vec{\alpha}_{AA} \cdot \vec{G}_s^i.
 \end{aligned} \tag{19}$$

The radial wave function includes all possible internal relative orbital angular momenta coupled to  $L = 0$ . It has also well-defined symmetry properties on the  $\vec{z}$  coordinate. Being  $P_{(12)(34)}(\vec{z} \rightarrow -\vec{z})R_{s_4}^i = P_z R_{s_4}^i$  one obtains,

$$\begin{aligned}
 P_{(12)(34)}R_1^i &= +R_1^i \\
 P_{(12)(34)}R_2^i &= -R_2^i \\
 P_{(12)(34)}R_3^i &= -R_3^i \\
 P_{(12)(34)}R_4^i &= +R_4^i.
 \end{aligned} \tag{20}$$

To evaluate radial matrix elements we use the notation introduced in Eq. (19):

$$\begin{aligned}
 \langle R_\gamma^i | f(x, y, z) | R_\beta^j \rangle &= \int_V (\vec{\alpha}_{S_\gamma} \cdot \vec{G}_s^i) f(x, y, z) (\vec{\alpha}_{S_\beta} \cdot \vec{G}_{s'}^j) dV \\
 &= \vec{\alpha}_{S_\gamma} \cdot F^{ij} \cdot \vec{\alpha}_{S_\beta},
 \end{aligned} \tag{21}$$

where  $\gamma$  and  $\beta$  stand for the symmetry of the radial wave function and  $F^{ij}$  is a matrix whose element  $(a, b)$  is defined through,

$$F_{ab}^{ij} = \int_V (\vec{G}_s^i)_a (\vec{G}_{s'}^j)_b f(x, y, z) dV, \tag{22}$$

being  $(\vec{G}_s^i)_a$  the component  $a$  of the vector  $\vec{G}_s^i$ . From Eq. (16) one obtains,

$$\begin{aligned}
 g(s_1, s_2, s_3)g(s'_1, s'_2, s'_3) &= \text{Exp}(-a_{ij}\bar{x}^2 - b_{ij}\bar{y}^2 - c_{ij}\bar{z}^2 \\
 &- \bar{s}_{ij}\bar{x} \cdot \bar{y} - \bar{e}_{ij}\bar{x} \cdot \bar{z} - \bar{f}_{ij}\bar{y} \cdot \bar{z}),
 \end{aligned} \tag{23}$$

where we have shortened the previous notation according to  $a_s^i \rightarrow a_i$ ,  $a_{ij} = a_i + a_j$  and  $\bar{d}_{ij} = (s_1 d_i + s'_1 d_j)$ . Therefore, all radial matrix elements will contain integrals of the form,

$$\begin{aligned}
 I &= \int_V \text{Exp}(-a_{ij}\bar{x}^2 - b_{ij}\bar{y}^2 - c_{ij}\bar{z}^2 - \bar{s}_{ij}\bar{x} \cdot \bar{y} \\
 &- \bar{e}_{ij}\bar{x} \cdot \bar{z} - \bar{f}_{ij}\bar{y} \cdot \bar{z}) f(x, y, z) d\bar{x}d\bar{y}d\bar{z},
 \end{aligned} \tag{24}$$

where the functions  $f(x, y, z)$  are the potentials. Being all of them radial functions (not depending on angular variables) one can solve the previous integral by noting:

$$\begin{aligned}
 &\int \text{Exp}\left[-\sum_{i,j=1}^n A_{ij}\bar{x}_i \cdot \bar{x}_j\right] f\left(\left|\sum \alpha_k \bar{x}_k\right|\right) d\bar{x}_1 \dots d\bar{x}_n \\
 &= \left(\frac{\pi^n}{\det A}\right)^{\frac{3}{2}} 4\pi \left(\frac{\Omega_{ij}}{\pi}\right)^{\frac{3}{2}} F(\Omega_{ij}, f),
 \end{aligned} \tag{25}$$

where

$$\begin{aligned} \frac{1}{\Omega_{ij}} &= \bar{\alpha} \cdot A^{-1} \cdot \alpha \\ F(A, f) &= \int e^{-Au^2} f(u)u^2 du \\ \det A &> 0 \\ \frac{1}{\Omega_{ij}} &> 0. \end{aligned} \tag{26}$$

One can extract some useful relations for the radial matrix elements using simple symmetry properties. Let us rewrite Eq. (21)

$$\begin{aligned} \langle R_\gamma^i | f(x, y, z) | R_\beta^j \rangle &= \langle R_{P_x P_y P_z}^i | f(x, y, z) | R_{P'_x P'_y P'_z}^j \rangle \\ &= \int_x \int_y \int_z R_{P_x P_y P_z}^i f(x, y, z) R_{P'_x P'_y P'_z}^j d\vec{x} d\vec{y} d\vec{z}. \end{aligned} \tag{27}$$

If  $f(x, y, z)$  depends only in one coordinate, for example  $\vec{x}$ , the integrals over the other coordinates will be zero if one of them has different symmetry properties,  $P_y \neq P'_y$  or  $P_z \neq P'_z$  in our example. Therefore

$$\begin{aligned} \langle R_\gamma^i | f(x) | R_\beta^j \rangle &\propto \delta_{\gamma\beta} \\ \langle R_\gamma^i | f(y) | R_\beta^j \rangle &\propto \delta_{\gamma\beta} \\ \langle R_\gamma^i | f(z) | R_\beta^j \rangle &\propto \delta_{\gamma\beta} \\ \langle R_\gamma^i | \text{Constant} | R_\beta^j \rangle &\propto \delta_{\gamma\beta}. \end{aligned} \tag{28}$$

The radial wave function described in this section is adequate to describe not only bound states, but also it is flexible enough to describe states of the continuum within a reasonable accuracy [50–52].

### 3. Two-body amplitudes

We have constructed the two-body amplitudes for all sub-systems entering the three- and four-body problems studied by solving the Lippmann–Schwinger equation of each  $(i, j)$  channel,

$$\begin{aligned} t^{ij}(p, p'; e) &= V^{ij}(p, p') + \int_0^\infty p''^2 dp'' V^{ij}(p, p'') \\ &\times \frac{1}{e - p''^2/2\mu} t^{ij}(p'', p'; e), \end{aligned} \tag{29}$$

where

$$V^{ij}(p, p') = \frac{2}{\pi} \int_0^\infty r^2 dr j_0(pr) V^{ij}(r) j_0(p'r), \tag{30}$$

and the two-body potentials consist of an attractive and a repulsive Yukawa term, *i.e.*,

$$V^{ij}(r) = -A \frac{e^{-\mu_A r}}{r} + B \frac{e^{-\mu_B r}}{r}. \tag{31}$$

The parameters of the  $\Lambda N$ ,  $\Xi N$ ,  $\Lambda\Lambda$  and  $\Xi\Xi$  channels were obtained by fitting the low-energy data and the phase shifts of each channel as given by the most recent update of the strangeness  $-1$  [19],  $-2$  [20] and  $-3$  and  $-4$  [30] ESC08c Nijmegen potentials. In the case of the  $NN$  interaction we use the Malfliet-Tjon models [53] with the parameters given in Ref. 54. The low-energy data and the parameters of these models are given in Table II. It is worth to note that the scattering length and effective range of the most recent update of the  $\Lambda\Lambda$  interaction derived from chiral effective field theories are very much like those of the ESC08c Nijmegen potential (see Table II of Ref. 42) unlike the earlier version used in Ref. 14 (see Table IV of Ref. 55) reporting remarkably small effective ranges.

TABLE II. Low-energy data and parameters of the local central Yukawa-type potentials given by Eq. (31) for the  $NN$  potential [54], and the most recent updates of the ESC08c Nijmegen interactions for the  $\Lambda N$  [19],  $\Xi N$  [20],  $\Xi\Xi$  [30], and  $\Lambda\Lambda$  [20] systems.

|                  | $(i, j)$           | $a(\text{fm})$ | $r_0(\text{fm})$ | $A(\text{MeV fm})$ | $\mu_A(\text{fm}^{-1})$ | $B(\text{MeV fm})$ | $\mu_B(\text{fm}^{-1})$ |
|------------------|--------------------|----------------|------------------|--------------------|-------------------------|--------------------|-------------------------|
| $NN$             | (1,0)              | -23.56         | 2.88             | 513.968            | 1.55                    | 1438.72            | 3.11                    |
| $\Lambda N$      | (1/2,0)            | -2.62          | 3.17             | 416                | 1.77                    | 1098               | 3.33                    |
|                  | (1/2,1)            | -1.72          | 3.50             | 339                | 1.87                    | 968                | 3.73                    |
| $\Xi N$          | (0,0) <sup>a</sup> | —              | —                | 120                | 1.30                    | 510                | 2.30                    |
|                  | (0,1)              | -5.357         | 1.434            | 377                | 2.68                    | 980                | 6.61                    |
|                  | (1,0)              | 0.579          | -2.521           | 290                | 3.05                    | 155                | 1.60                    |
|                  | (1,1)              | 4.911          | 0.527            | 568                | 4.56                    | 425                | 6.73                    |
| $\Xi\Xi$         | (0,1)              | 0.53           | 1.63             | 210                | 1.60                    | 560                | 2.05                    |
|                  | (1,0)              | -7.25          | 2.00             | 155                | 1.75                    | 490                | 5.60                    |
| $\Lambda\Lambda$ | (0,0)              | -0.853         | 5.126            | 121                | 1.74                    | 926                | 6.04                    |

<sup>a</sup>This channel is discussed on Sec. III.

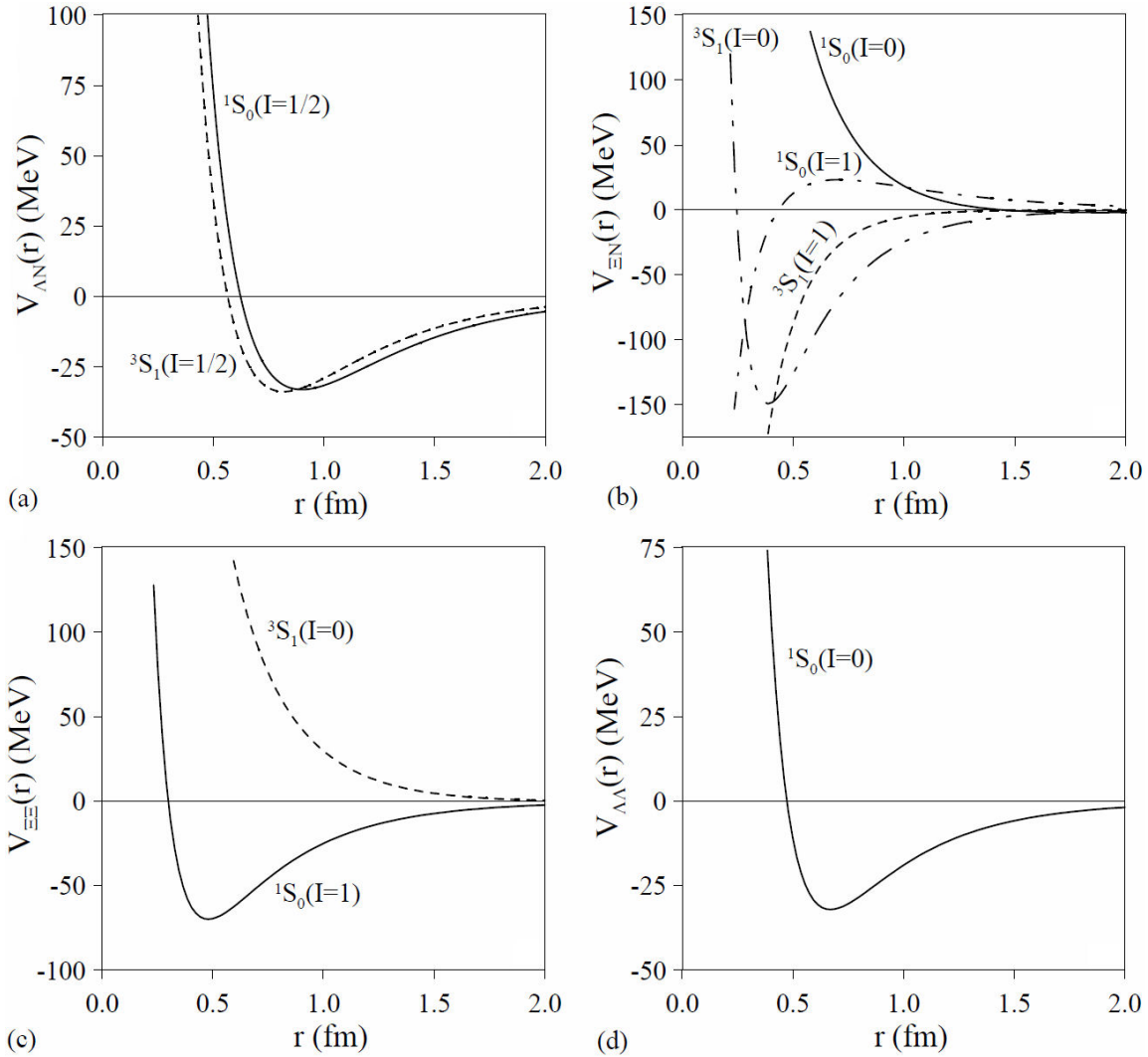


FIGURE 1. (a)  $V_{\Lambda N}(r)$  potential as given by Eq. (31) with the parameters of Table II. (b) Same as (a) for the  $V_{\Xi N}(r)$  potential. (c) Same as (a) for the  $V_{\Xi\Xi}(r)$  potential. (d) Same as (a) for the  $V_{\Lambda\Lambda}(r)$  potential.

TABLE III. Two-body  $NN$ ,  $YN$  and  $YY$  isospin-spin  $(i, j)$  channels that contribute to a given three- or four-body state with total isospin  $I$  and total spin  $J$ . The last column indicates the corresponding threshold for each state, that would come given by  $\sum_{i=1}^{3(4)} M_i - E$ , where  $M_i$  are the masses of the baryons of each channel,  $B_1$  stands for the binding energy of the deuteron and  $B_2$  for the binding energy of the  $D^*$   $\Xi N$  state.

|                     | $(I, J)$     | $\Lambda N$       | $\Xi N$                   | $\Xi\Xi(NN)$  | $\Lambda\Lambda$ | $E$    |
|---------------------|--------------|-------------------|---------------------------|---------------|------------------|--------|
| $\Xi NN$            | $(1/2, 1/2)$ | –                 | $(0,0),(0,1),(1,0),(1,1)$ | $(0,1),(1,0)$ | –                | $B_1$  |
|                     | $(1/2, 3/2)$ | –                 | $(0,1),(1,1)$             | $(0,1)$       | –                | $B_1$  |
|                     | $(3/2, 1/2)$ | –                 | $(1,0),(1,1)$             | $(1,0)$       | –                | $B_2$  |
|                     | $(3/2, 3/2)$ | –                 | $(1,1)$                   | –             | –                | $B_2$  |
| $\Xi\Xi N$          | $(1/2, 1/2)$ | –                 | $(0,0),(0,1),(1,0),(1,1)$ | $(0,1),(1,0)$ | –                | $B_2$  |
|                     | $(1/2, 3/2)$ | –                 | $(0,1),(1,1)$             | $(0,1)$       | –                | $B_2$  |
|                     | $(3/2, 1/2)$ | –                 | $(1,0),(1,1)$             | $(1,0)$       | –                | $B_2$  |
|                     | $(3/2, 3/2)$ | –                 | $(1,1)$                   | –             | –                | $B_2$  |
| $\Xi\Xi NN$         | $(2, 0)$     | –                 | $(1,0),(1,1)$             | $(1,0)$       | –                | $2B_2$ |
| $\Lambda\Lambda NN$ | $(1, 0)$     | $(1/2,0),(1/2,1)$ | –                         | $(1,0)$       | $(0,0)$          | 0      |

The  $\Xi N$   $^1S_0$  ( $I = 0$ ) potential was fitted to the  $\Xi N$  phase shifts given in Fig. 14 of Ref. 20 without taking into account the inelasticity, *i.e.*, assuming  $\rho = 0$  (this two-body channel does not contribute to the three- and four-body bound states found in this work). Regarding the two-body interactions containing a single  $\Lambda$ , they are constrained by a simultaneous fit to the combined  $NN$  and  $YN$  scattering data, supplied with constraints on the  $YN$  and  $YY$  interaction originating from the G-matrix information on hypernuclei [19].

The potentials obtained are shown in Fig. 1. In Fig. 1(a) we show the  $V_{\Lambda N}(r)$  potential that it is tightly constrained by the existing experimental data. The interaction is attractive at intermediate range and strongly repulsive at short range, but without having bound states. In Fig. 1(b) we show the  $V_{\Xi N}(r)$  potential, where one notes the attractive character of the  $^3S_1$  ( $I = 1$ )  $\Xi N$  partial wave, giving rise to the  $D^*$  bound state [18] with a binding energy of 1.6 MeV. We also confirm how all the  $J = 1$  and  $I = 1$   $\Xi N$  interactions are attractive<sup>iii</sup> [30]. Regarding the  $\Xi\Xi$  interaction, Fig. 1(c), we observe the attractive character of the  $^1S_0$  ( $I = 1$ ) potential, that although having bound states in earlier versions of the ESC08c Nijmegen potential [34], in the most recent update of the strangeness  $-4$  sector it does not present a bound state [30]. The existence of bound states in the  $\Xi\Xi$  system has been predicted by different calculations in the literature [35–37]. It can be definitively stated that all models agree on the fairly important attractive character of this channel, either with or without a bound state [38]. Finally, in Fig. 1(d) we show the  $V_{\Lambda\Lambda}(r)$  potential, mainly determined by the  $NN$  and  $YN$  data, and SU(3) symmetry [20, 21]. It gives account of the pivotal results of strangeness  $-2$  physics, the NAGARA [22] and the KISO [18] events. Although other double- $\Lambda$  hypernuclei events, like the DEMACHIYANAGI and HIDA events [43], are not explicitly taken into account, the G-matrix nuclear matter study of  $\Xi^-$  capture both in  $^{12}\text{C}$  and  $^{14}\text{N}$  (see section VII of Ref. 20), concludes that the  $\Xi N$  attraction in the ESC08c potential is consistent with the  $\Xi$ -nucleus binding energies given by the emulsion data of the twin  $\Lambda$ -hypernuclei.

#### 4. Results and discussion

Let us first of all show the reliability of the input potentials. We compare in Fig. 2 the  $\Lambda N$  and  $\Lambda\Lambda$  phase shifts reported by the ESC08c Nijmegen potential and those obtained by our fits with the two-body potentials of Eq. (31) and the parameters given in Table II. As can be seen the agreement is good. As stated above, the  $\Xi N$   $^1S_0$  ( $I = 0$ ) potential was fitted to the  $\Xi N$  phase shifts given in Fig. 14 of Ref. 20. Once we have described the phase shifts, the  $\Lambda N$  and  $\Lambda\Lambda$  potentials include in an effective manner the coupling to other two-body channels as it may be the  $\Sigma N$  or  $\Xi N$  two-body systems<sup>iv</sup>. We have also tested the two-body interactions in the three-body problem of systems made of  $N$ 's and  $\Lambda$ 's. The hypertriton is bound by 144 keV, and the  $\Lambda nn$  system is unbound.

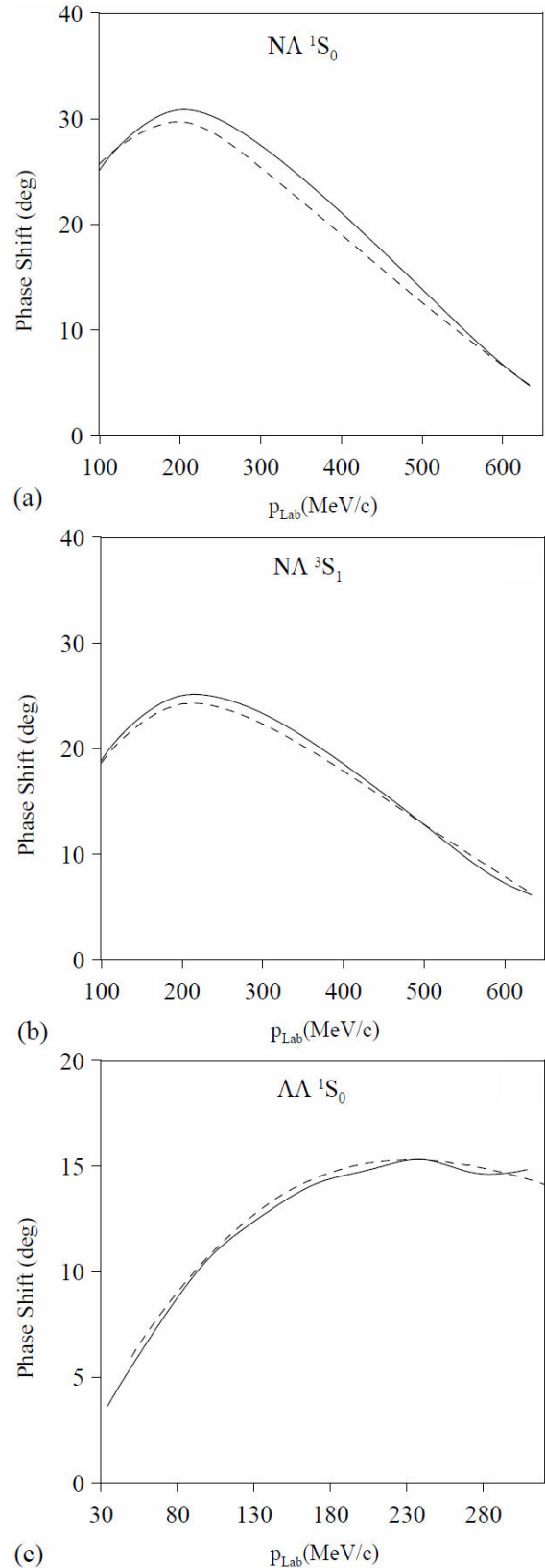


FIGURE 2. (a)  $\Lambda N$   $^1S_0$  phase shifts. The solid line stands for the results of the ESC08c Nijmegen potential and the dashed line for the results of the two-body potential of Eq. (31) with the parameters given in Table II. (b) Same as (a) for the  $\Lambda N$   $^3S_1$  phase shifts. (c) Same as (a) for the  $\Lambda\Lambda$   $^1S_0$  phase shifts.

The reasonable description of the known two- and three-body problems gives confidence to address the study of other three- and four-body systems. We show in Table III the channels of the different two-body subsystems contributing to each  $(I, J)$  three- and four-body state that we will study. For the  $\Xi\Xi NN$  system we only consider the  $I = 2$  channels, because the  $I = 0$  and 1 states would decay strongly to  $\Lambda\Lambda NN$  states. The three- and four-body problems are studied by means of the ESC08c Nijmegen interactions described in Sec. 3 and given in Table II. The binding energies are measured with respect to the lowest threshold, indicated in Table III for each particular state.

#### 4.1. Three-body systems

We show in Fig. 3 the Fredholm determinant of all  $\Xi NN$  channels [59,60]. As we can see in Fig. 3(b), a bound state is found for the  $(I)J^P = (3/2)1^+/2$   $\Xi NN$  state, 1.3 MeV be-

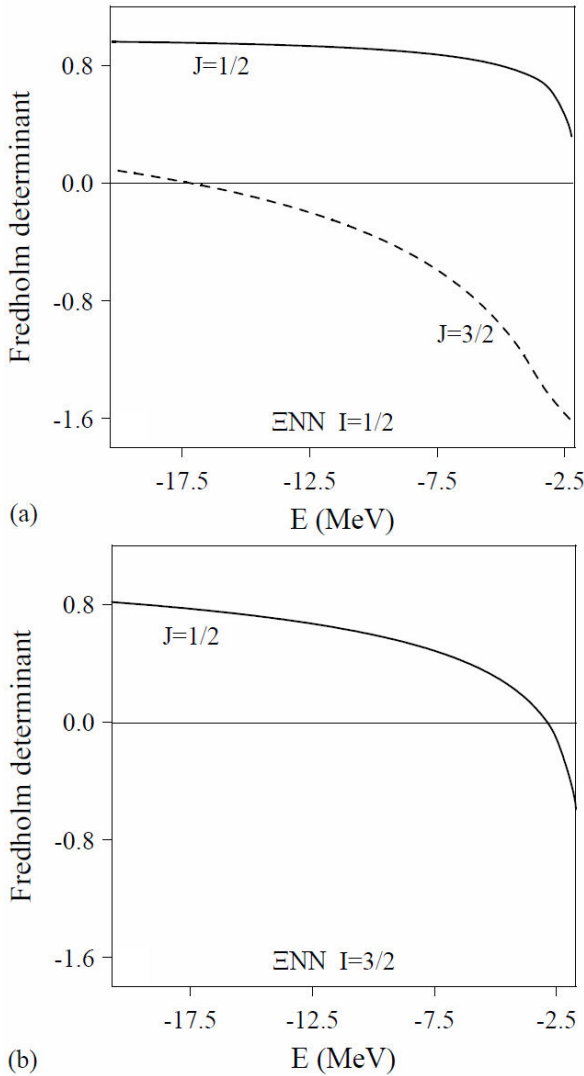


FIGURE 3. (a) Fredholm determinant for the  $J = 1/2$  and  $J = 3/2$   $I = 1/2$   $\Xi NN$  channels. (b) Fredholm determinant for the  $J = 1/2$   $I = 3/2$   $\Xi NN$  channel.

low the corresponding threshold,  $2m_N + m_\Xi - B_2$ , where  $B_2$  is the binding energy of the  $D^* \Xi N$  state. However, the most interesting result of the  $\Xi NN$  system is shown in Fig. 3(a), the very large binding energy of the  $(1/2)3^+/2$  state, which would make it easy to identify experimentally as a sharp resonance lying some 17.2 MeV below the  $\Xi NN$  threshold. The  $\Lambda\Lambda - \Xi N$   $(i, j) = (0, 0)$  transition channel, which is responsible for the decay  $\Xi NN \rightarrow \Lambda\Lambda N$ , does not contribute to the  $(I)J^P = (1/2)3^+/2$  state in a pure  $S$ -wave configuration [60]. One would need at least the spectator nucleon to be in a  $D$ -wave or that the  $\Lambda\Lambda - \Xi N$  transition channel be in one of the negative parity  $P$ -wave channels, with the nucleon spectator also in a  $P$ -wave. Thus, due to the angular momentum barriers the resulting decay width of the  $(1/2)3^+/2$  state is expected to be very small.

For the  $\Xi NN$  three-baryon system with  $(I, J) = (3/2, 3/2)$ , only the  $(i, j) = (1, 1)$   $\Xi N$  channel contributes (see Table III), and the corresponding Faddeev equations with two identical fermions can be written as [27],

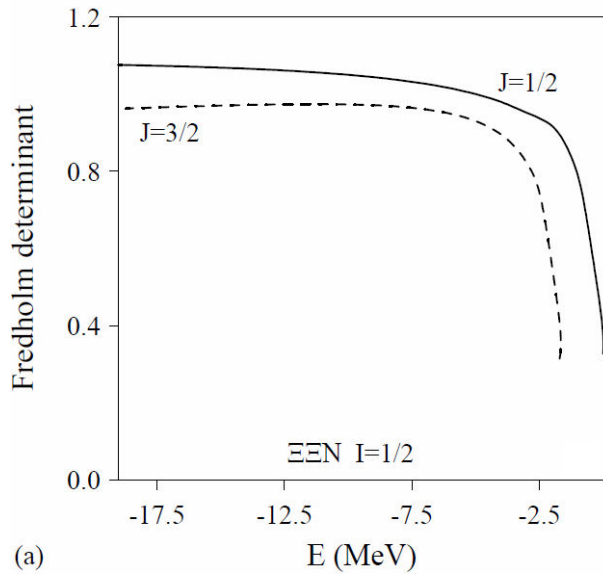
$$T = -t_N^{\Xi} G_0 T. \quad (32)$$

Thus, due to the negative sign in the r.h.s. the  $\Xi N$  interaction is effectively repulsive and, therefore, no bound state is possible in spite of the attraction of the  $\Xi N$  subsystem. The minus sign in Eq. (32) is a consequence of the identity of the two nucleons since the first term of the r.h.s. of Eq. (32) proceeds through  $\Xi$  exchange and it corresponds to a diagram where the initial and final states differ only in that the two identical fermions have been interchanged which brings the minus sign. This effect has been pointed out before [61]. This is the reason why the Fredholm determinant for the  $(I, J) = (3/2, 3/2)$   $\Xi NN$  channel is not shown in Fig. 3(b).

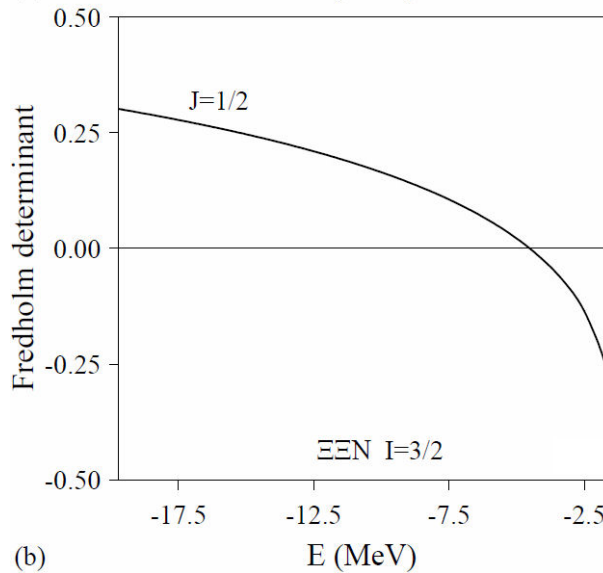
Finally, we show in Fig. 4 the Fredholm determinant of all  $\Xi\Xi N$  channels. The Fredholm determinant for the  $(I)J^P = (3/2)3/2^+$  channel is not shown in Fig. 4(b) for the same reason explained above for the  $\Xi NN$  system, it is strongly repulsive. In the  $\Xi\Xi N$  system there appears a bound state with quantum numbers  $(I)J^P = (3/2)1^+/2$ , 2.9 MeV below the lowest threshold,  $2m_\Xi + m_N - B_2$ , where  $B_2$  stands for the binding energy of the  $D^* \Xi N$  subsystem. Since this  $\Xi\Xi N$  state has isospin 3/2 it can not decay into  $\Xi\Lambda\Lambda$  due to isospin conservation so that it would be stable. This stable state appears in spite of the fact that the last update of the ESC08c Nijmegen  $\Xi\Xi$   $^1S_0(I = 1)$  potential has not bound states, as it is however predicted by several models in the literature. If bound states would exist for the  $\Xi\Xi$  system the three-body state would become deeply bound as it happens for the  $\Xi NN$  system. The  $I = 1/2$  channels are also attractive but they are not bound.

Let us finally mention that our results for three-body systems containing a  $\Xi N$  subsystem has been recently reproduced by means of the configuration-space Faddeev equations [62].





(a)



(b)

FIGURE 4. (a) Fredholm determinant for the  $J = 1/2$  and  $J = 3/2$   $I = 1/2$   $\Xi\Xi N$  channels. (b) Fredholm determinant for the  $J = 1/2$   $I = 3/2$   $\Xi\Xi N$  channel.

#### 4.2. Four-body systems

In the previous section we have seen that all three-body systems made of  $N$ 's and  $\Xi$ 's in the maximal isospin channel, *i.e.*, systems consisting only of neutrons and negative  $\Xi$ 's or protons and neutral  $\Xi$ 's, are bound. As mentioned above, the uniqueness of these systems is a consequence of the two-body interactions between  $NN$ ,  $\Xi N$  and  $\Xi\Xi$  pairs being all in the isospin 1 channel. Thus, the strong decay  $\Xi N \rightarrow \Lambda\Lambda$  is forbidden. Therefore, such states, if bound, would be stable under the strong interaction. This is why we now proceed to study four-body systems made of  $N$ 's and  $\Xi$ 's in the maximal isospin channel,  $I = 2$ . The most favorable configuration to minimize the effect of the Pauli principle is the  $\Xi\Xi NN$  system, that due to identity of two  $N$ 's and two  $\Xi$ 's can only exist with  $J = 0$  [63].

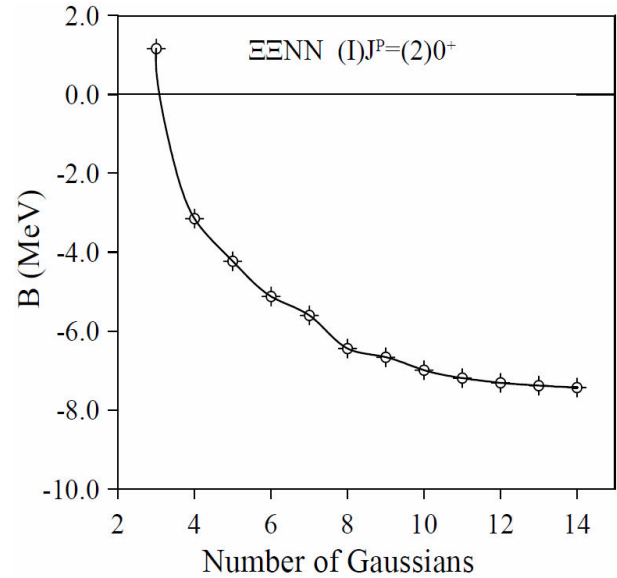


FIGURE 5. Binding energy of the  $(I)J^P = (2)0^+$   $\Xi\Xi NN$  state as a function of the number of Gaussians in the variational calculation.

The binding energy of the  $\Xi\Xi NN$  state has been calculated by means of the variational method with generalized Gaussians described in Sec. 2. The method has been used in the four-body sector to study the possible existence of tetraquarks [64–66] and tested against the hyperspherical harmonic formalism with comparable results [51, 52]. We show in Fig. 5 the binding energy of the  $(I)J^P = (2)0^+$   $\Xi\Xi NN$  state as a function of the number of Gaussians in the variational calculation. As we can see the result is almost stable considering 12 Gaussians, although we have pushed further our calculation with a negligible gain of binding in the second decimal digit. The lowest threshold for this state is  $2B_2 = 3.2$  MeV, where  $B_2$  is the binding energy of the  $D^*$   $\Xi N$  state (see Table III). Thus, the state lies 7.4 MeV below the  $\Xi\Xi NN$  mass, with a separation energy of 4.2 MeV with respect to an asymptotic state made of two  $D^*$   $\Xi N$  dibaryons.

One can also study the behavior of the root mean square radius (RMS) of the four-body system, defined in the usual way,

$$\begin{aligned} \text{RMS} &= \left( \frac{\sum_{i=1}^4 m_i \langle (\vec{r}_i - \vec{R}_{CM})^2 \rangle}{\sum_{i=1}^4 m_i} \right)^{1/2} \\ &= \frac{1}{2} \left( \frac{\langle r_{NN}^2 \rangle}{1 + m_{\Xi}/m_N} + \langle r_{\Xi\Xi}^2 \rangle \frac{m_{\Xi}/m_N}{1 + m_{\Xi}/m_N} \right. \\ &\quad \left. + \langle r_{NN-\Xi\Xi}^2 \rangle \frac{m_{\Xi}/m_N}{(1 + m_{\Xi}/m_N)^2} \right)^{1/2}. \end{aligned} \quad (33)$$

The results are shown in Fig. 6, where besides the RMS radius we have also calculated the root mean square radii of the different Jacobi coordinates. As seen in Table III, only the  $^1S_0(I = 1)$   $NN$  and  $\Xi\Xi$  channels contribute to the

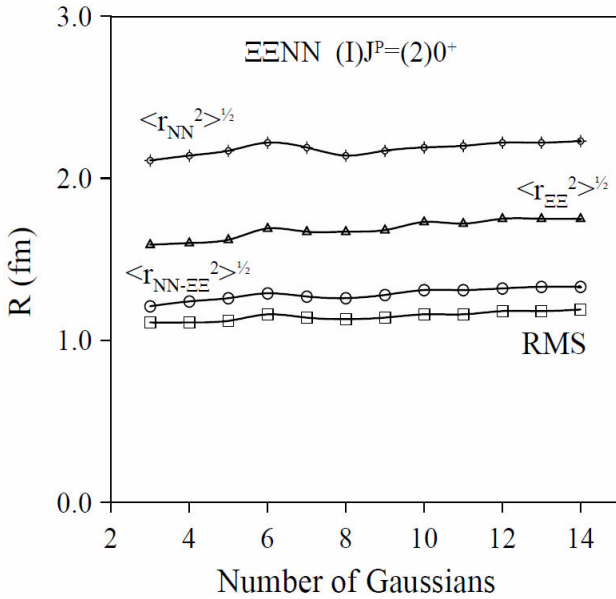


FIGURE 6. Root mean square radii of the  $(I)J^P = (2)0^+$   $\Xi\Xi NN$  state as a function of the number of Gaussians in the variational calculation. See text for details.

$(I)J^P = (2)0^+$   $\Xi\Xi NN$  state. As discussed in Sec. 3, although they are attractive, the  $^1S_0(I=1)$   $NN$  and  $\Xi\Xi$  channels do not present a bound state, giving the largest internal radii. In the  $\Xi N$  subsystem one finds contributions from the  $^1S_0(I=1)$  and  $^3S_1(I=1)$  channels, the last one presenting the  $D^*$  bound state, which is the responsible of the smallest radius in the  $\Xi - N$  relative coordinate. The RMS gets fully stabilized with 14 Gaussians with a value of 1.18 fm.

We have finally evaluated the binding energy of the  $\Lambda\Lambda NN$  system with quantum numbers  $(I)J^P = (1)0^+$  [67]. The system is unbound appearing just above threshold and thus it does not seem to be Borromean, a four-body bound state without two- or three-body stable subsystems. An unbound result was also reported in Ref. 68, although in this case the authors made use of repulsive gaussian-type potentials for any of the two-body subsystems (see the figure on pag. 475) what does not allow for the existence of any bound state.

We have studied the dependence of the binding on the strength of the attractive part of the different two-body interactions entering the four-body problem. For this purpose we have used the following interactions,

$$V^{B_1 B_2}(r) = -g_{B_1 B_2} A \frac{e^{-\mu_A r}}{r} + B \frac{e^{-\mu_B r}}{r} \quad (34)$$

with the same parameters given in Table II. The system hardly gets bound for a reasonable increase of the strength of the  $\Lambda\Lambda$ ,  $g_{\Lambda\Lambda}$ , interaction. Although one cannot exclude that the genuine  $\Lambda\Lambda$  interaction in dilute states as the one studied here could be slightly stronger than the one reported in Ref. 20, however, one needs  $g_{\Lambda\Lambda} \geq 1.8$  to get a bound state, what would destroy the agreement with the ESC08c Nijmegen  $\Lambda\Lambda$  phase shifts. Note also that this is a very sensitive parameter for the study of double- $\Lambda$  hypernuclei [40] and

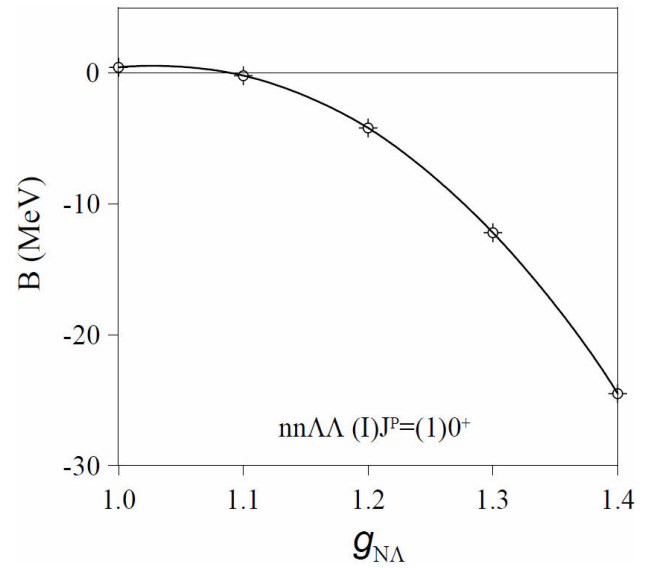


FIGURE 7. Binding energy of the  $(I)J^P = (1)0^+$   $nn\Lambda\Lambda$  state as a function of the multiplicative factor,  $g_{N\Lambda}$ , in the attractive part of  $V^{N\Lambda}(r)$  interaction for  $g_{NN} = g_{\Lambda\Lambda} = 1$ .

this modification would produce an almost  $\Lambda\Lambda$  bound state in free space, in particular it would give rise to  $a_{1S_0}^{\Lambda\Lambda} = -29.15$  fm and  $r_{01S_0}^{\Lambda\Lambda} = 1.90$  fm. The four-body system would also become bound taking a factor 1.2 in the  $NN$  interaction. However, such modification would make the  $^1S_0$   $NN$  potential as strong as the  $^3S_1$  [53] and thus the singlet  $S$ -wave would develop a dineutron bound state,  $a_{1S_0}^{NN} = 6.07$  fm and  $r_{01S_0}^{NN} = 1.96$  fm. The situation is slightly different when dealing with the  $\Lambda N$  interaction. We have used a common factor  $g_{N\Lambda}$  for attractive part of the two  $\Lambda N$  partial waves,  $^1S_0$  and  $^3S_1$ . We show in Fig. 7 the binding energy of the  $(I)J^P = (1)0^+$   $\Lambda\Lambda NN$  state as a function of the multiplicative factor  $g_{N\Lambda}$ , for  $g_{NN} = g_{\Lambda\Lambda} = 1$ . As one can see the four-body system develops a bound state for  $g_{N\Lambda} = 1.1$ , giving rise to the  $\Lambda N$  low-energy parameters:  $a_{1S_0}^{\Lambda N} = -5.60$  fm,  $r_{01S_0}^{\Lambda N} = 2.88$  fm,  $a_{3S_1}^{\Lambda N} = -2.91$  fm, and  $r_{03S_1}^{\Lambda N} = 2.99$  fm, far from the values constrained by the existing experimental data.

Reference 14 tackled the same problem by fitting low-energy parameters of older versions of the Nijmegen-RIKEN potential [30, 69] or chiral effective field theory [55, 70], by means of a single Yukawa attractive term or a Morse parametrization. The method used to solve the four-body problem is similar to the one we have used in our calculation, thus the results might be directly comparable. Our improved description of the two- and three-body subsystems and the introduction of the repulsive barrier for the  $^1S_0$   $NN$  partial wave, relevant for the study of the triton binding energy (see Table II of Ref. 71), leads to a four-body state just above threshold, that cannot get bound by a reliable modification in the two-body subsystems. As clearly explained in Ref. 14, the window of Borromean binding is more and more reduced for potentials with harder inner cores.

## 5. Summary

This manuscript intends to summarize our recent work on few-body systems made of  $N$ 's,  $\Lambda$ 's and  $\Xi$ 's based on the most recent updates of the ESC08c Nijmegen potential in the different strangeness sectors, accounting for the recent experimental information. We have solved the three- and four-body bound state problems by means of Faddeev equations and a generalized Gaussian variational method, respectively. The hypertriton,  $np\Lambda$  ( $I$ ) $J^P=(1/2)1/2^+$ , is bound by 144 keV, and the recently discussed  $nm\Lambda$  ( $I$ ) $J^P=(1/2)1/2^+$  system is unbound. We have found that the  $\Xi NN$  system presents bound states with quantum numbers ( $I$ ) $J^P=(3/2)1/2^+$  and ( $I$ ) $J^P=(1/2)3/2^+$ , the last one being a deeply bound state lying 15 MeV below the  $\Xi d$  threshold. The  $\Xi\Xi N$  system presents a bound state with quantum numbers ( $I$ ) $J^P=(3/2)1/2^+$ , in spite of having used the most recent update of the ESC08c Nijmegen potential that does not predict  $\Xi\Xi$  bound states. In the case of the three-

body systems we note that there appear bound states in all systems made of  $N$ 's and  $\Xi$ 's with maximal isospin. The same conclusion has been obtained in the four-body system, concluding a  $\Xi\Xi NN$  bound state with quantum numbers ( $I$ ) $J^P = (2)0^+$ , lying 7.4 MeV below the  $\Xi\Xi NN$  threshold with a root mean square radius of 1.18 fm. We have also studied the ( $I$ ) $J^P = (1)0^+$   $\Lambda\Lambda NN$  state, it does not present a bound state. Thus, the  ${}^4_{\Lambda\Lambda}n$  four-body system does not seem to be Borromean.

## Acknowledgments

This work has been partially funded by COFAA-IPN (México), by Ministerio de Economía, Industria y Competitividad and EU FEDER under Contracts No. FPA2016-77177 and FPA2015-69714-REDT, by Junta de Castilla y León under Contract No. SA041U16, by Generalitat Valenciana PrometeoII/2014/066, and by USAL-FAPESP grant 2015/50326-5.

- 
- i.* Note that the pronounced cusp-like structure seen in many  $\Lambda N$  related observables near the  $\Sigma N$  threshold could be very well a signature of a dibaryon [25].
  - ii.* Being the  $N$  and  $\Xi$   $I = 1/2$  particles, an analogous table serves for the symmetry properties of the wave function in isospin space. In the case of the  $\Lambda$ 's the isospin wave function is symmetric.
  - iii.* There are also models for the strangeness  $-2$  baryon-baryon interaction based on EFT calculations [55] showing  $I = 1$   $\Xi N$  attraction, although one cannot conclude the strength of the interaction due to the huge effective ranges reported.
  - iv.* Although by fitting the  $\Lambda N$  phase shifts, the coupling to the  $\Sigma N$  system has been included in an effective manner, it would also be interesting to unfold the effective  $\Lambda N$  interaction, separating the contribution from  $\Lambda N \leftrightarrow \Sigma N$ . As it has been discussed in the literature [9, 10, 27, 56–58] the hypertriton does not get bound by considering only  $\Lambda NN$  channels, but it is necessary to include also  $\Sigma NN$  channels. Similar considerations hold for the  $\Lambda\Lambda \leftrightarrow \Xi N$  coupling.
1. P. Demorest, T. Pennucci, S. Ransom, M. Roberts, and J. Hesses, *Nature* **467** (2010) 1081.
  2. J. Antoniadis *et al.*, *Science* **340** (2013) 1233232.
  3. S. Weissenborn, D. Chatterjee, and J. Schaffner-Bielich, *Phys. Rev. C* **85** (2012) 065802 [Erratum *Phys. Rev. C* **90** (2014) 019904(E)].
  4. D. Lonardonì, F. Pederiva, and S. Gandolfi, *Phys. Rev. C* **89** (2014) 014314.
  5. K. A. Maslov, E. E. Kolomeitsev, and D. N. Voskresensky, *Phys. Lett. B* **748** (2015) 369.
  6. Y. Yamamoto, E. Hiyama, and Th. A. Rijken, EPJ Web of Conferences **3** (2010) 07007.
  7. E. Hiyama, Y. Yamamoto, T. Motoba, Th. A. Rijken, and M. Kamimura, *Phys. Rev. C* **78** (2008) 054316.
  8. M. Yamaguchi, K. Tominaga, Y. Yamamoto, and T. Ueda, *Prog. Theor. Phys.* **105** (2001) 627.
  9. H. Garcilazo and A. Valcarce, *Phys. Rev. C* **89** (2014) 057001.
  10. E. Hiyama, S. Ohnishi, B.F. Gibson, and Th. A. Rijken, *Phys. Rev. C* **89** (2014) 061302(R).
  11. A. Gal and H. Garcilazo, *Phys. Lett. B* **736** (2014) 93.
  12. S.-I. Ando, U. Raha, and Y. Oh, *Phys. Rev. C* **92** (2015) 024325.
  13. I. R. Afnan and B. F. Gibson, *Phys. Rev. C* **92** (2015) 054608.
  14. J.-M. Richard, Q. Wang, and Q. Zhao, *Phys. Rev. C* **91** (2015) 014003.
  15. C. Rappold *et al.*, *Phys. Rev. C* **88** (2013) 041001(R).
  16. H. Garcilazo and A. Valcarce, *Phys. Rev. Lett.* **110** (2013) 012503.
  17. H. Garcilazo, *Phys. Rev. C* **93** (2016) 024001.
  18. K. Nakazawa *et al.*, *Prog. Theor. Exp. Phys.* (2015) 033D02.
  19. M.M. Nagels, Th. A. Rijken, and Y. Yamamoto, arXiv:1501.06636.
  20. M.M. Nagels, Th. A. Rijken, and Y. Yamamoto, arXiv:1504.02634.
  21. Th.A. Rijken and H.-F. Schulze, *Eur. Phys. J. A* **52** (2016) 21.
  22. H. Takahashi *et al.*, *Phys. Rev. Lett.* **87** (2001) 212502.
  23. T. Nagae, *Prog. Theor. Phys. Supp.* **185** (2010) 299.
  24. A. Gal, E.V. Hungerford, and D.J. Millener, *Rev. Mod. Phys.* **88** (2016) 035004.
  25. H. Machner *et al.*, *Nucl. Phys. A* **901** (2013) 65.
  26. A. Esser *et al.*, *Phys. Rev. Lett.* **114** (2015) 232501.
  27. H. Garcilazo, T. Fernández-Caramés, and A. Valcarce, *Phys. Rev. C* **75** (2007) 034002.

28. H Garcilazo, A. Valcarce, and T. Fernández-Caramés, *Phys. Rev. C* **76** (2007) 034001.
29. T. Harada and Y. Hirabayashi, *Phys. Rev. C* **89** (2014) 054603.
30. Th.A. Rijken, M.M. Nagels, and Y. Yamamoto, *Few-Body Syst.* **54** (2013) 801.
31. K. Sasaki *et al.*, *Prog. Theor. Exp. Phys.* (2015) 113B01.
32. E. Hiyama, M. Kamimura, Y. Yamamoto, T. Motoba, and Th.A. Rijken, *Prog. Theor. Phys. Supp.* **185** (2010) 152.
33. T.F. Caramés and A. Valcarce, *Phys. Rev. C* **85** (2012) 045202.
34. V.G.J. Stoks and T.A. Rijken, *Phys. Rev. C* **59** (1999) 3009.
35. J. Haidenbauer and U. -G. Meissner, *Phys. Lett. B* **684** (2010) 275.
36. S.R. Beane *et al.*, *Phys. Rev. D* **85** (2012) 054511.
37. G.A. Miller, *Chin. J. Phys.* **51** (2013) 466.
38. J. Haidenbauer, Ulf.-G. Meissner, and S. Petschauer, *Eur. Phys. J. A* **51** (2015) 17.
39. S. R. Beane *et al.*, *Phys. Rev. D* **80** (2009) 074501.
40. H. Nemura, Y. Akaishi, and K.S. Myint, *Phys. Rev. C* **67** (2003) 051001(R).
41. Y. Fujiwara, Y. Suzuki, and C. Nakamoto, *Prog. Part. Nucl. Phys.* **58** (2007) 439.
42. J. Haidenbauer, Ulf.-G. Meissner, and S. Petschauer, *Nucl. Phys. A* **954** (2016) 273.
43. K. Nakazawa (KEK-E176, E373 and J-PARC-E07 Collaborations), *Nucl. Phys. A* **835** (2010) 207.
44. K. Nakazawa and H. Takahashi, *Prog. Theor. Phys. Supp.* **185** (2010) 335.
45. T. Nagae *et al.*, *J-PARC E05 experiment. Proposal for J-PARC 50 GeV Proton Synchrotron: Spectroscopic Study of  $\Xi$ -Hypernucleus,  $^{12}_{\Xi}\text{Be}$ , via the  $^{12}\text{C}(K^-, K^+)$  Reaction*; available at: [http://j-parc.jp/researcher/Hadron/en/pac\\_0606/pdf/p05-Nagae.pdf](http://j-parc.jp/researcher/Hadron/en/pac_0606/pdf/p05-Nagae.pdf), (2015).
46. K. Nakazawa *et al.*, *Phys. Proc.* **80** (2015) 69.
47. H. Garcilazo and A. Valcarce, *Phys. Rev. C* **93** (2016) 064003.
48. I.R. Afnan and A.W. Thomas, *Phys. Rev. C* **10** (1974) 109.
49. H. Garcilazo and T. Mizutani, in  *$\pi NN$  Systems* (World Scientific, Singapore, 1990).
50. Y. Suzuki and K. Varga, *Lect. Not. Phys. M* **54** (1998) 1.
51. J. Vijande and A. Valcarce, *Symmetry* **1** (2009) 155.
52. J. Vijande and A. Valcarce, *Phys. Rev. C* **80** (2009) 035204.
53. R.A. Malfliet and J.A. Tjon, *Nucl. Phys. A* **127** (1969) 161.
54. J.L. Friar *et al.*, *Phys. Rev. C* **42** (1990) 1838.
55. H. Polinder, J. Haidenbauer, and U.-G. Meissner, *Phys. Lett. B* **653** (2007) 29.
56. K. Miyagawa, H. Kamada, W. Glöckle, and V. Stoks, *Phys. Rev. C* **51** (1995) 2905.
57. B. F. Gibson and D. R. Lehman, *Phys. Rev. C* **16** (1977) 1679.
58. B.F. Gibson and D.R. Lehman, *Nucl. Phys. A* **329** (1979) 308.
59. H. Garcilazo and A. Valcarce, *Phys. Rev. C* **92** (2015) 014004.
60. H. Garcilazo and A. Valcarce, *Phys. Rev. C* **93** (2016) 034001.
61. H. Garcilazo, *J. Phys. G* **13** L63. (1987).
62. I. Filikhin, V.M. Suslov, and B. Vlahovic, *Math. Mod. Geom.* **2** (2017) 1.
63. H. Garcilazo, A. Valcarce, and J. Vijande, *Phys. Rev. C* **94** (2016) 024002.
64. J. Vijande, A. Valcarce, and J.-M. Richard, *Phys. Rev. D* **76** (2007) 114013.
65. J. Vijande, A. Valcarce, and N. Barnea, *Phys. Rev. D* **79** (2009) 074010.
66. T.F. Caramés, A. Valcarce, and J. Vijande, *Phys. Lett. B* **699** (2011) 291.
67. H. Garcilazo, A. Valcarce, and J. Vijande, *Chin. Phys. C* **41** (2017) 074102.
68. M.L. Lekala, G.J. Rampho, R.M. Adam, S.A. Sofianos, and V.B. Belyaev, *Phys. of Atom. Nucl.* **77** (2014) 472.
69. Th.A. Rijken, M.M. Nagels, and Y. Yamamoto, *Prog. Theor. Phys. Supp.* **185** (2010) 14.
70. J. Haidenbauer *et al.*, *Nucl. Phys. A* **915** (2013) 24.
71. R.A. Malfliet and J.A. Tjon, *Ann. of Phys.* **61** (1970) 425.